
Development and Verification of Conditions for Ductile Tearing Instability and Arrest

Prepared by J. A. Joyce

U.S. Naval Academy

Prepared for
U.S. Nuclear Regulatory
Commission

B603100561 B6022B
PDR NUREG
CR-4528 R PDR

NOTICE

This report was prepared as an account of work sponsored by an agency of the United States Government. Neither the United States Government nor any agency thereof, or any of their employees, makes any warranty, expressed or implied, or assumes any legal liability of responsibility for any third party's use, or the results of such use, of any information, apparatus, product or process disclosed in this report, or represents that its use by such third party would not infringe privately owned rights.

NOTICE

Availability of Reference Materials Cited in NRC Publications

Most documents cited in NRC publications will be available from one of the following sources:

1. The NRC Public Document Room, 1717 H Street, N.W.
Washington, DC 20555
2. The Superintendent of Documents, U.S. Government Printing Office, Post Office Box 37082,
Washington, DC 20013-7082
3. The National Technical Information Service, Springfield, VA 22161

Although the listing that follows represents the majority of documents cited in NRC publications, it is not intended to be exhaustive.

Referenced documents available for inspection and copying for a fee from the NRC Public Document Room include NRC correspondence and internal NRC memoranda, NRC Office of Inspection and Enforcement bulletins, circulars, information notices, inspection and investigation notices, Licensee Event Reports; vendor reports and correspondence; Commission papers; and applicant and licensee documents and correspondence.

The following documents in the NUREG series are available for purchase from the GPO Sales Program: formal NRC staff and contractor reports, NRC-sponsored conference proceedings, and NRC booklets and brochures. Also available are Regulatory Guides, NRC regulations in the *Code of Federal Regulations*, and *Nuclear Regulatory Commission Issuances*.

Documents available from the National Technical Information Service include NUREG series reports and technical reports prepared by other federal agencies and reports prepared by the Atomic Energy Commission, forerunner agency to the Nuclear Regulatory Commission.

Documents available from public and special technical libraries include all open literature items, such as books, journal and periodical articles, and transactions. *Federal Register* notices, federal and state legislation, and congressional reports can usually be obtained from these libraries.

Documents such as theses, dissertations, foreign reports and translations, and non NRC conference proceedings are available for purchase from the organization sponsoring the publication cited.

Single copies of NRC draft reports are available free, to the extent of supply, upon written request to the Division of Technical Information and Document Control, U.S. Nuclear Regulatory Commission, Washington, DC 20555.

Copies of industry codes and standards used in a substantive manner in the NRC regulatory process are maintained at the NRC Library, 7920 Norfolk Avenue, Bethesda, Maryland, and are available there for reference use by the public. Codes and standards are usually copyrighted and may be purchased from the originating organization or, if they are American National Standards, from the American National Standards Institute, 1430 Broadway, New York, NY 10018.

Development and Verification of Conditions for Ductile Tearing Instability and Arrest

Manuscript Completed: February 1986
Date Published: February 1986

Prepared by
J. A. Joyce

U.S. Naval Academy
Annapolis, MD 21402

Prepared for
Division of Engineering Technology
Office of Nuclear Regulatory Research
U.S. Nuclear Regulatory Commission
Washington, D.C. 20555
NRC FIN B7026

ABSTRACT

The objective of this work was to take an in depth look at the process of ductile tearing instability and especially to evaluate experimentally the conditions for arrest of a ductile tearing instability. A secondary objective was to evaluate the sensitivity of a ductile tearing instability arrest to rate at which it occurred and to the material rate sensitivity. Major conclusions are that the ductile tearing instability initiates slowly but in a mechanical spring apparatus it approaches drop tower crack growth rate conditions and hence the phenomena is effected by the material rate sensitivity. The conditions necessary for arrest are completely stated and demonstrated by experimental data on a 3 percent Ni structural steel.

TABLE OF CONTENTS

	<u>Page</u>
Abstract	iii
Table of Contents	v
List of Figures	vii
Prior Reports	ix
Introduction	1
1.0 <u>Description of the Experimental Tests</u>	1
1.1 Apparatus	1
1.2 Material	4
2.0 <u>Analysis</u>	4
2.1 Tearing Instability Theory	4
2.2 Key Curve Theory	6
2.3 Validation of the Key Curve Formula	8
3.0 <u>Presentation of the Results</u>	8
3.1 Static Results	8
3.2 Instability Tests	12
3.3 Application of the Key Curve Method	12
4.0 <u>Discussion</u>	19
4.1 Conditions for Tearing Instability Arrest	19
4.2 Effects of Rate	19
4.3 Application of Additional Mass	19
4.4 Applicability of "Computer Compliant" Tests	21
4.5 Prediction of a Crack Arrest	21
5.0 <u>Conclusions</u>	21
Bibliography	22
Acknowledgement	24

LIST OF FIGURES

<u>No.</u>	<u>Page</u>
1. Specimen drawing for a 1T Compact Specimen.	2
2. Schematic of the spring compliant test apparatus as used for the instability tests.	3
3. Figures showing a) the load displacement records for six specimens with different crack lengths and b) the resulting key curve form.	9
4. Figure showing the agreement of the assumed power law key curve with static unloading compliance data.	10
5. Baseline static J-R curves tested to very large crack extensions for prediction of $T_{material}$	11
6. Typical instability data showing the usual static data defining instability and subsequent arrest.	13
7. A combination of both static and rapid instability test data compared to baseline static load displacement data.	14
8. A comparison of tearing instability J-R curves obtained by the key curve method and baseline static J-R curves.	16
9. J-T plot showing the observed point of tearing instability.	17
10. A load displacement plot showing the energy balance required for the arrest of a ductile tearing instability.	18
11. Plots of COD versus time shown for light and increased mass tests showing typical test velocities achieved.	20

PRIOR REPORTS

Prior reports in this series are listed below:

1. J. A. Joyce, "Application of the Key Curve Method to Determining J-R Curves for A533B Steel," NUREG/CR-1290, U.S. Naval Academy, Annapolis, MD (February 1980).
2. J. P. Gudas, M. G. Vassilaros, J. A. Joyce, D. A. Davis, and D. R. Anderson, "A Summary of Recent Investigations of Compact Specimen Geometry Effects on the J_1 -R Curve of High-Strength Steels," NUREG/CR-1813, DTNSRDC, Annapolis, MD (November 1980).
3. J. A. Joyce, "Instability Testing of Compact and Pipe Specimens Utilizing a Test System Made Compliant by Computer Control," NUREG/CR-2257, U.S. Naval Academy, Annapolis, MD (March 1982).
4. J. A. Joyce, "Static and Dynamic J-R Curve Testing of A533B Steel Using the Key Curve Analysis Technique," NUREG/CR-2274, U.S. Naval Academy, Annapolis, MD (July 1981).
5. M. G. Vassilaros, J. P. Gudas and J. A. Joyce, "Experimental Investigation of Tearing Instability Phenomena for Structural Materials," NUREG/CR-2570, DTNSRDC, Annapolis, MD (Revised August 1982).

Introduction

This project follows a series of work in the area of ductile tearing instability reported earlier (1-3). In the previous work it was demonstrated that the point of onset of ductile tearing instability could be accurately predicted for compact and circumferentially cracked pipes using the Paris(4) tearing criterion. It was also demonstrated that a compliant test machine could be developed either by adding mechanical springs or by programming a computer controlled servo-hydraulic test machine to produce equivalent flexible loading conditions. Two differences were observed between the computer controlled test and the mechanical spring system. The first difference was that the time duration of the instability was much shorter for the mechanical spring test than for the computer controlled test because of the slow response of the minicomputer that was used. Also, in crack opening terms, the instability arrest occurred much sooner in the computer controlled test than in the mechanical spring test.

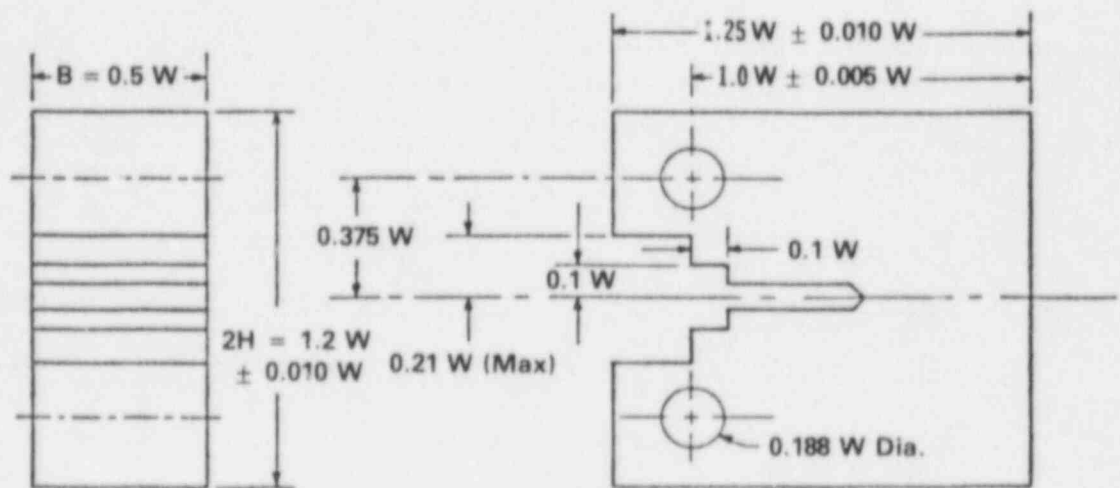
The second difference was ascribed to the fact that in the mechanical system energy could be dissipated only by being absorbed by the specimen (with some minor friction losses) while in the computer controlled system, energy can pass into the servohydraulic system. The result was that the computer controlled system produced ductile crack arrest when load and tearing modulus conditions were satisfied while the mechanical spring system required that tearing stability be reestablished, but also that a balance of energy released by the spring apparatus and absorbed by the specimen be reestablished.

The objective of this project was to clarify the process of ductile crack arrest by measuring the required quantities during the crack arrest phenomena, to check more accurately this energy balance, to look for rate effects on the crack arrest and to establish a complete statement of the conditions required for the arrest of a ductile tearing crack.

1.0 Description of The Experimental Tests

1.1 Apparatus

All tests were carried out on 1T compact specimens as shown in Fig 1. These specimens were essentially standard J-R curve test specimens as recommended by reference(5). The apparatus used is shown schematically in Fig 2 and has some important modifications when compared to apparatus used previously for tearing instability tests(1-3,6). First a load link was used to measure the load transmitted to the specimen which was directly coupled to the specimen in contrast to previous experiments where the load cell was usually on the opposite side of the spring system from the specimen. Second, a capability is present in this apparatus to apply additional mass to vary the rate of instability after instability initiation. Third, a high speed digital oscilloscope is present to record the load versus load line displacement record during the instability and instability arrest. Aside from these changes the apparatus is essentially just a rather standard computer aided J-R curve test apparatus as outlined in previous work utilizing a mechanical spring of variable stiffness to produce ductile tearing instabilities.



Compact Test Specimen for Pin of $0.1875 W (+ 0.000 W / - 0.001 W)$ Diameter

Figure 1. Specimen drawing for a 1T compact specimen.

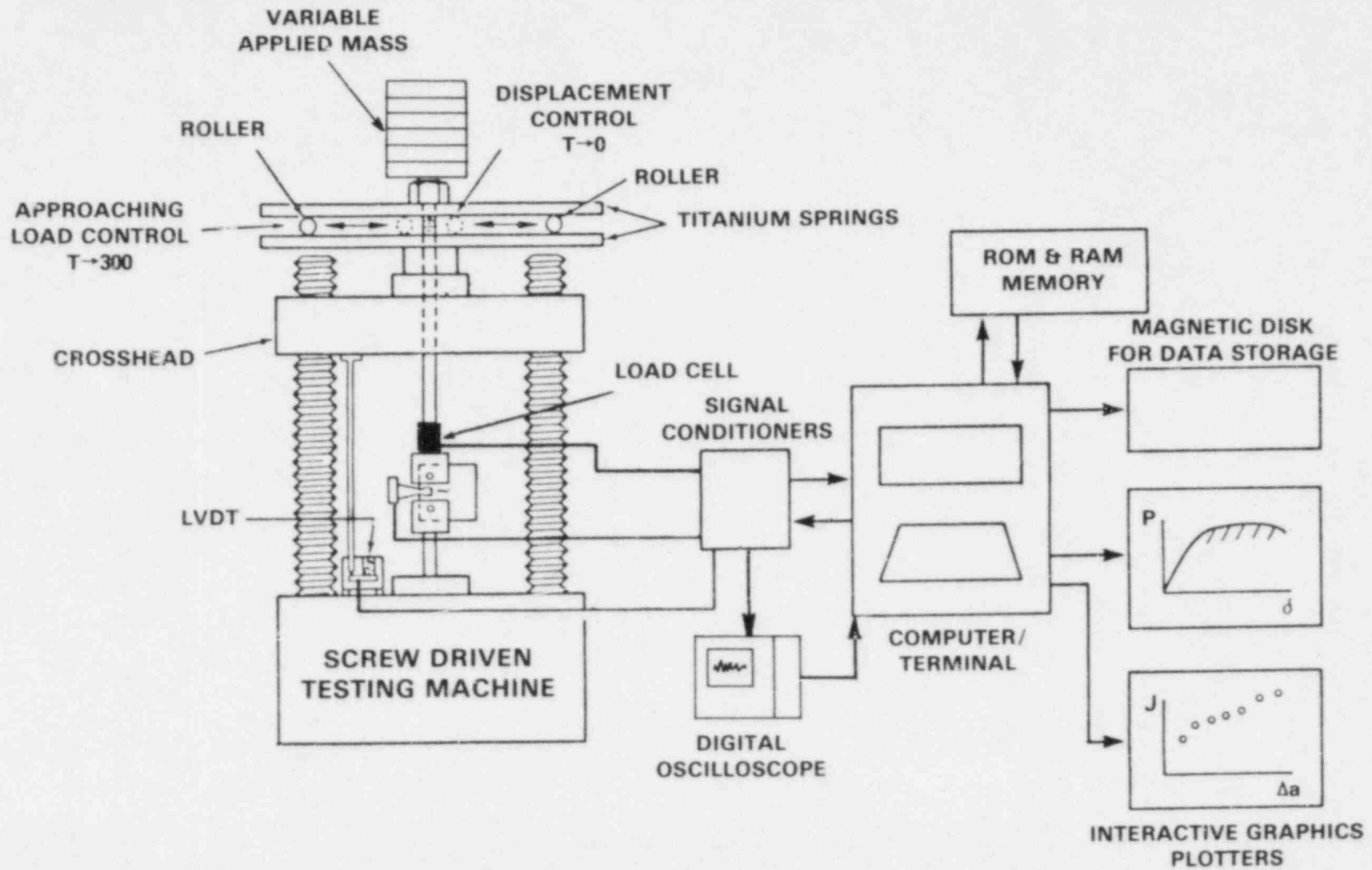


Figure 2. Schematic of the spring compliant test apparatus as utilized for compact specimens.

1.2 Material

The material used for the investigation was provided in the form of a 38mm (1.5 inch) thick plate. The chemical composition for the plate is shown in Table 1. All tests were conducted with the notches in the T-L orientation. Tensile test data obtained on standard 0.505 inch-2 inch gage length tensile specimens loaded in the transverse direction using a slow test speed gave the following properties:

$$\sigma_{UTS} = 731 \text{ MPa (105 ksi)},$$

$$\sigma_y = 614 \text{ MPa (89 ksi)},$$

$$\% \text{ elongation} = 23$$

$$\% \text{ reduction of area} = 63$$

2.0 Analysis

2.1 Tearing Instability Theory

The tearing instability theory of Paris, et. al.(4) states that a flawed member will tear stably when it has a J_{applied} greater than J_{IC} , an applied load at its limit load and a T_{applied} greater than the material capacity, T_{material} . The T_{material} can be obtained from the formula:

$$T_{\text{material}} = \frac{E}{\sigma_0^2} \frac{dJ}{da} \quad (1)$$

where

$$E = \text{material elastic modulus}$$

$$\sigma_0 = \text{material flow stress}$$

$$dJ/da = \text{slope of material J-R curve at the } J_{\text{applied}} \text{ value}$$

The T_{applied} quantity is a function of the specimen geometry, type of loading, and test machine or structural stiffness.

Calculations of T_{applied} have been accomplished for several important cases and are available in the literature(4,7-10). For this project the analysis of Ernst et.al.(10) is used which assumes that the family of load displacement curves for a compact specimen can be written in the form:

$$P = kg(a/W) h(\text{COD}/W) \quad (2)$$

and develops an expression for T_{applied} of the form

$$T_{\text{applied}} = \frac{E}{\sigma_0^2} \left\{ -\gamma \frac{J}{b} + \frac{\eta^2}{b^2} P \left(\frac{1}{\frac{h'}{Wh} + \frac{KM}{P}} \right) \right\} \quad (3)$$

TABLE 1 - CHEMICAL COMPOSITION OF STEEL USED FOR J-R CURVE TESTING

Identification	Chemical Composition (wt%)										
	C	Mn	P	S	Cu	Si	Ni	CR	Mo	V	Ti
3 Ni Steel (FYB)	.153	.33	.012	.013	.033	.18	2.55	1.66	.37	.033	Less than .001

where

$$\gamma = 1 + .76 b/W$$

$$\eta = 2 + .522 b/W$$

K_M = machine stiffness

$$h' = dh/d(COD/W)$$

$$b = W-a$$

W = specimen width.

The actual form of the load displacement curve used in this work was:

$$P = k \alpha b (COD/W)^n \quad (4)$$

where

$$\alpha = \sqrt{4 \left(\frac{a}{b}\right)^2 + 4 \left(\frac{a}{b}\right) + 2} - 2 \frac{a}{b} - 1 \quad (5)$$

from the Green and Hundy(11) limit load solution applied to the CT specimen.

k, n = fitting coefficients chosen here to fit the experimental data.

To obtain J-R curves directly from specimen load displacement curves a "key curve" analysis is used as first presented by Joyce et. al.(12).

2.2 Key Curve Theory

In this analysis a key curve is defined by a function $F1$ containing only units of stress of the form

$$\frac{PW}{Bb^2} = F1 \left(\frac{\Delta}{W}, \frac{a}{W}, \frac{H}{W}, \frac{B}{W}, \text{material properties} \right) \quad (6)$$

where H and B are specimen dimensions, Δ = COD, and the other quantities are as defined above.

In terms of the $F1$ or key curve function J can be expressed as

$$J = - \int_0^{\Delta} \left(\frac{b^2}{W^2} \frac{\partial F1}{\partial (a/W)} - \frac{2b}{W} F1 \right) d\Delta \quad (7)$$

Taking the differential of J assuming only a and COD change and reintegrating gives:

$$dJ = \left[\frac{2b}{W} F1 - \frac{b^2}{W^2} \frac{\partial F1}{\partial (a/W)} \right] d\Delta + \left[- \int_0^{\Delta} \frac{2}{W} F1 d\Delta \right. \\ \left. + \int_0^{\Delta} \frac{4b}{W^2} \frac{\partial F1}{\partial (a/W)} d\Delta - \int_0^{\Delta} \frac{b^2}{W^3} \frac{\partial^2 F1}{\partial (a/W)^2} d\Delta \right] da \quad (8)$$

Using a similar procedure an equation for crack growth increments can be obtained in the form:

$$da = \frac{\frac{b^2}{W^2} \frac{\partial F1}{\partial (a/W)} d\Delta - dP}{\frac{2b}{W} F1 - \frac{b^2}{W^2} \frac{\partial F1}{\partial (a/W)}} \quad (9)$$

Substituting the assumed form of the load versus COD curves from equation (4) and substituting it into the key curve form of equation (6) gives

$$F1 = \frac{PW}{Bb^2} = \frac{\alpha kW}{Bb} \left(\frac{COD}{W} \right)^n \quad (10)$$

and from this the derivatives required to evaluate equations (8) and (9) can be obtained as follows:

$$\frac{\partial F1}{\partial (COD/W)} = \frac{nk\alpha W}{Bb} \left(\frac{COD}{W} \right)^{n-1} \quad (11)$$

$$\frac{\partial F1}{\partial (a/W)} = \frac{k}{B} \left(\frac{COD}{W} \right)^n \left\{ \frac{\frac{4a/W}{(1-a/W)^2} + \frac{2}{(1-a/W)}}{4 \left(\frac{a/W}{1-a/W} \right)^2 + 4 \left(\frac{a/W}{1-a/W} \right) + 2} - \frac{2}{1-a/W} + \alpha \right\} \quad (12)$$

with $\frac{b^2}{W^3} \frac{\partial^2 F1}{\partial (a/W)^2} \cong 0$ in comparison with other terms. (13)

Application of these equations to obtain J-R curves is described in the following sections.

It is also shown by Ernst et. al.(10) that $T_{material}$ can be expressed as:

$$T_{material} = \frac{E}{\sigma_0^2} \left\{ -\gamma \frac{J}{b} + \frac{n^2}{b^2} P \left(\frac{1}{\frac{h'}{Wh} - \frac{1}{P} \frac{dP}{dCOD}} \right) \right\} \quad (14)$$

for a compact specimen for which COD is also the load line displacement. It should then be apparent that $T_{material}$ exceeds $T_{applied}$ as long as K_M exceeds $\left| \frac{dP}{dCOD} \right|$ and that instability should occur when the slope of the specimen load displacement curve falls below the stiffness of the test system being used. This is a very convenient way to look at tearing instability when complete load displacement records are available.

2.3 Validation of the Key Curve Formula

Various types of key curves have been used by various authors (3,10,11,12). Some have been purely experimental and others have used different measures of fit to experimental data. Verification of the applicability of the form chosen here to the compact specimen is demonstrated in Fig 3 where a series of load versus COD records are first shown in a standard way and then replotted in a dimensionless fashion in which the a/W dependence is removed so that all curves fall on a single line up to the point of crack initiation. This result clearly demonstrates that the a/W dependence assumed in equation (4) is accurate for the present specimen and material combination.

To demonstrate that a power law fit is accurate for the COD dependence for this specimen and material combination the result shown in Fig. 4 was generated from the two unloading compliance baseline specimen run as a part of this test program. The ordinate quantity, $P/(Bk\alpha)$ was updated as far as crack length dependence after each unloading and this results in a sawtooth shape for the curves shown. The upper envelope of this plot corresponds well with a function of the form $k(COD/W)^n$ and a fit with $k = 1558.MPa$ and $n = 0.18$ is shown on Fig. 4.

3.0 Presentation of the Results

3.1 Static Results

Static J-R curves were run as baseline data using the single specimen unloading compliance technique presented by Joyce and Gudas(13). The resulting J-R curves are shown in Fig 5 for two of these samples. These tests were run far beyond the present limits given by the recommended procedure of Albrecht et. al.(5) but nonetheless straight J-R curves resulted beyond J_{IC} and there is every

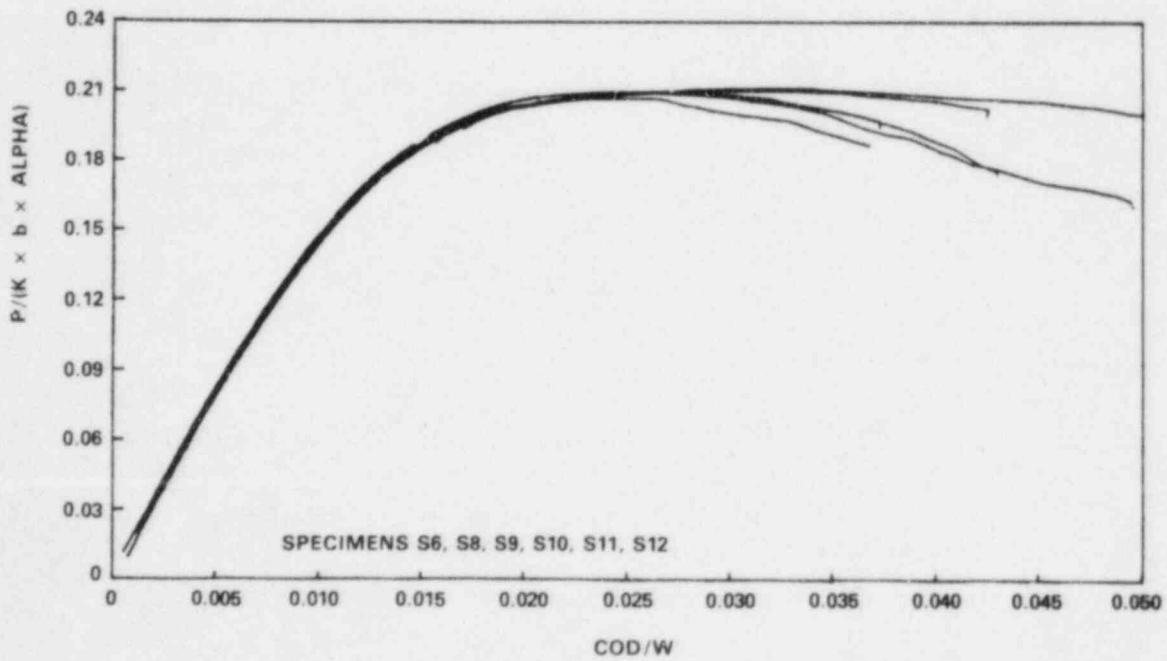
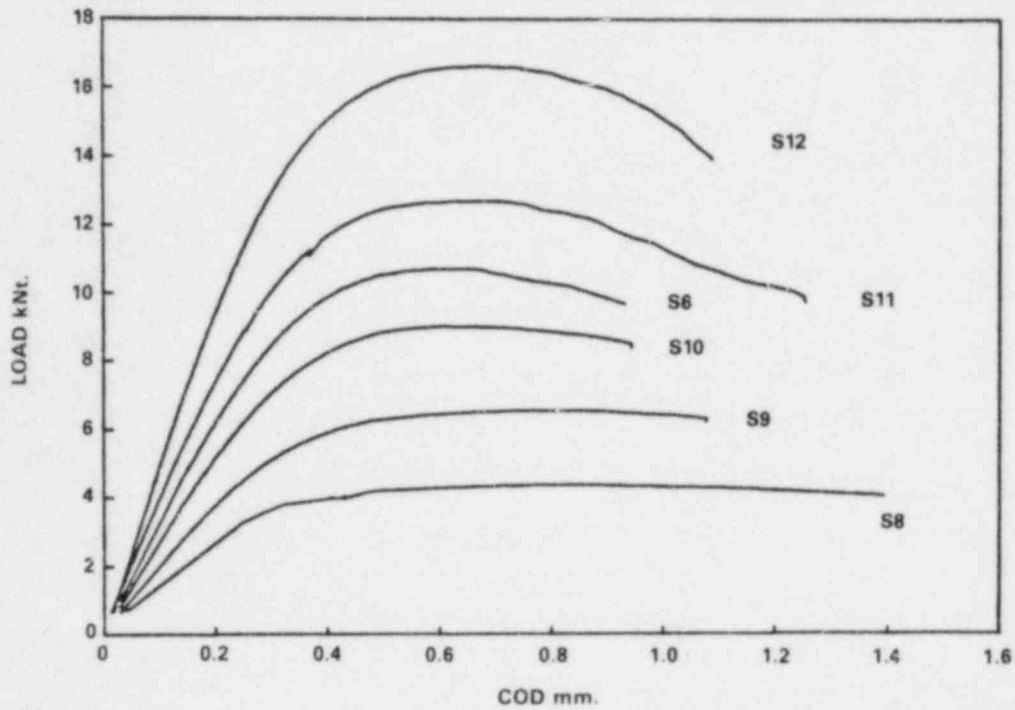


Figure 3. Figures showing a) the load displacement records for six specimens with different crack lengths and b) the resulting key curve form.

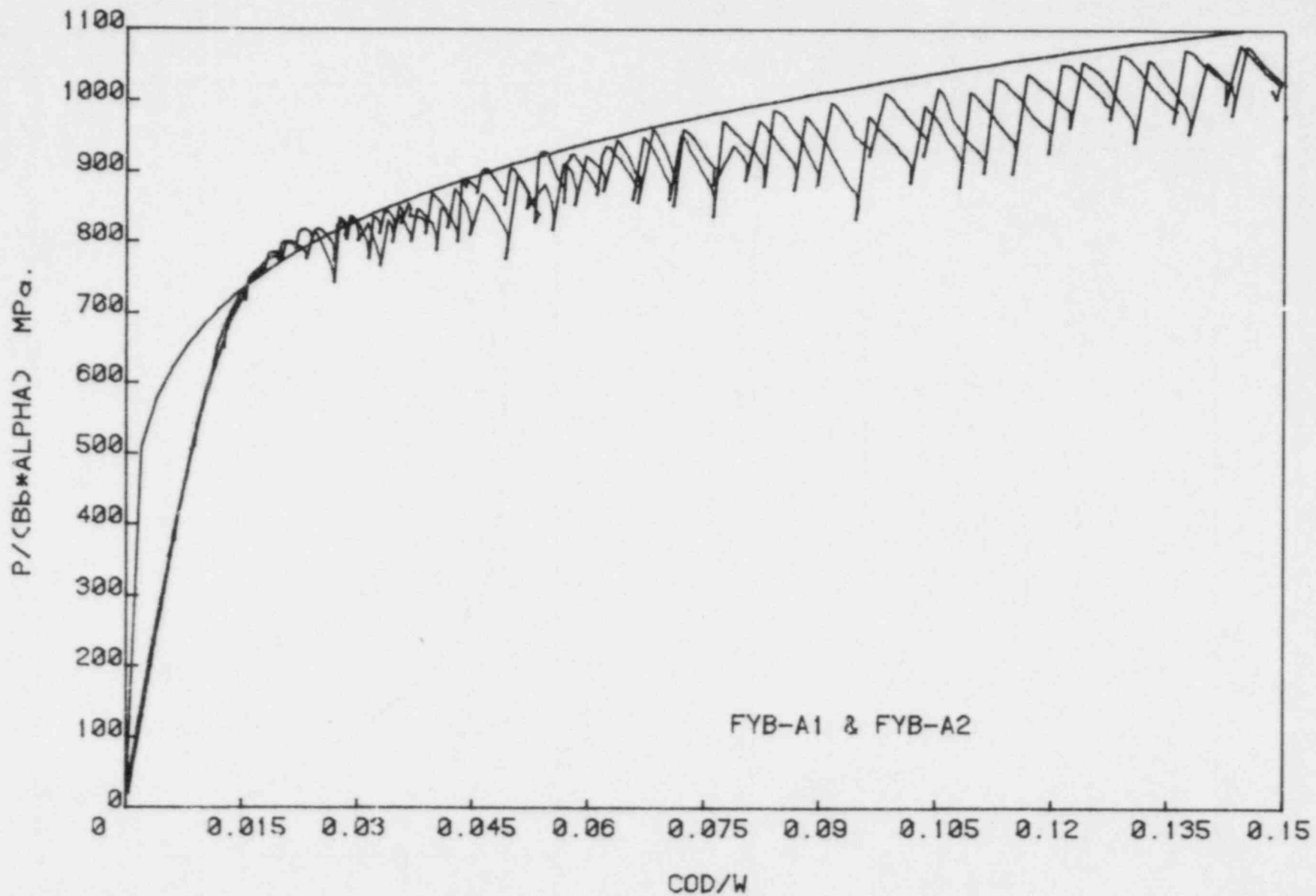


Figure 4. Figure showing the agreement of the assumed power law key curve with static unloading compliance data.

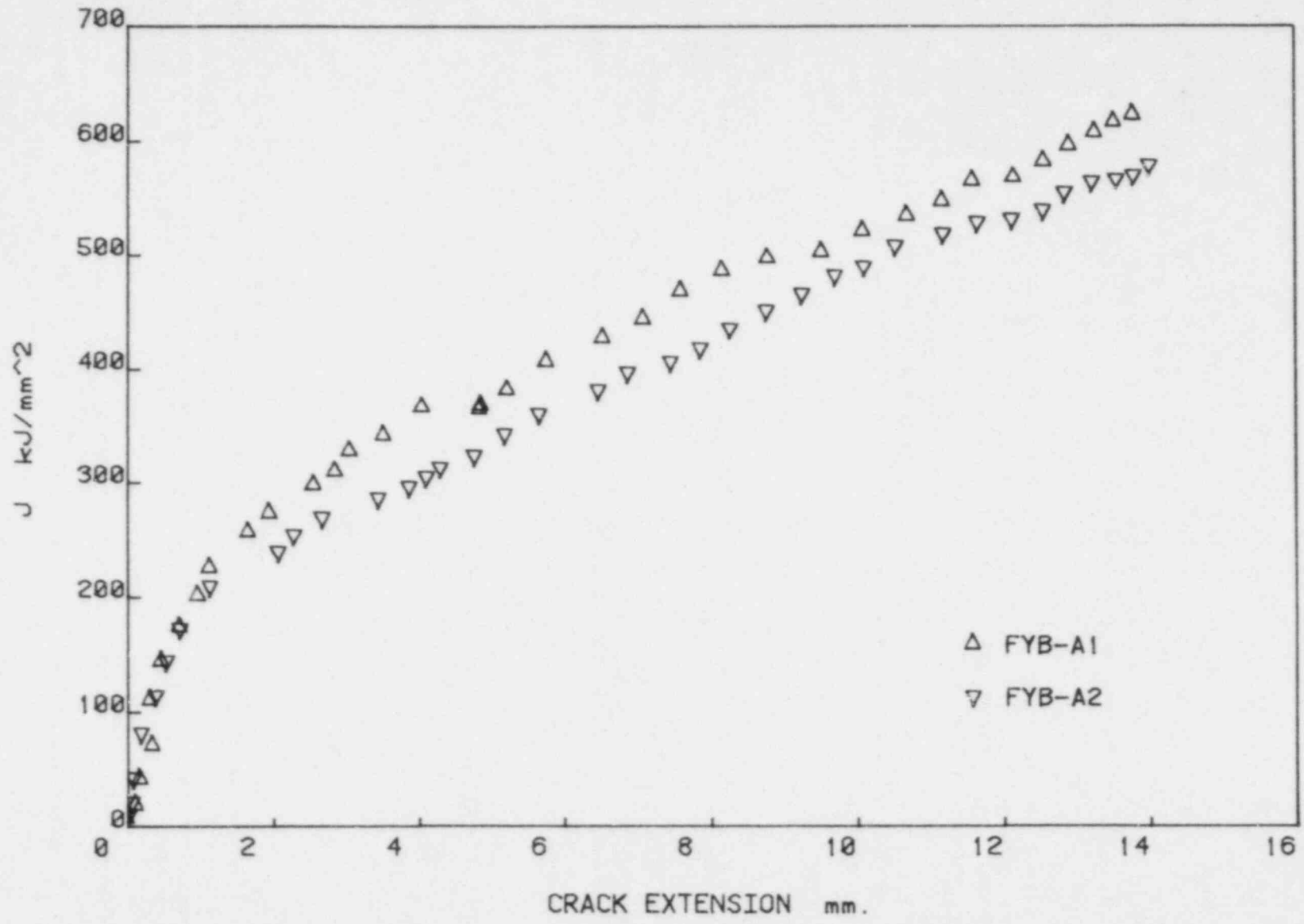


Figure 5. Baseline static J-R curves tested to very large crack extensions for prediction of T_{material}

reason to believe the J-R curves are accurate for tearing instability verification throughout their full extent.

3.2 Instability Tests

The apparatus was then changed to include the spring fixtures described previously and tests were run which were interrupted by tearing instabilities as shown in Fig 6. For these tests data was obtained by the digital voltmeter/scanner system both before and after the instability and by the Nicolet oscilloscope during the instability and combined data files were assembled after the test completion.

Fig 7 shows a comparison of a load displacement curve obtained statically with one resulting from the instability interrupted tests. The instability tests match the static tests until the point of instability, but then they run higher through to the completion of the test. This is a real effect and was further verified by post test optical measurements of specimen crack lengths (see Table 2) which shows that rapid (instability) tests produced less crack extension than static tests at the COD value of 0.30 inches at which all tests were stopped.

3.3 Application of the Key Curve Method

Application of the key curve analysis of equations (8) and (9) to the rapid load displacement curves results in the calculation of J-R curves which are shown in Fig 8 along with the baseline static J-R curves. Final measured crack lengths on these specimens were from 0.494 to 0.506 as shown in Table 3 and the key curve function exponent n was chosen as 0.25 to give these results using the key curve analysis and an iterative process. Clearly the elevation of these J-R curves above the static baseline data is expected because of the elevated load displacement records like that of Fig 7, but also because of the smaller crack lengths present in these specimens at a given applied COD.

Fig 9 shows a typical J-T plot for one of the instability tests. Because data is in hand through the full instability process complete $T_{applied}$ and $T_{material}$ curves can be plotted on this figure. The J- $T_{material}$ curves were obtained here by fitting a power law curve of the form

$$J = A(\Delta a)^m \quad (15)$$

to the J-R curve data of Figure 8 beyond J_{IC} and differentiating to obtain dJ/da . Clearly the initiation point is accurately predicted using this analysis (four cases were run) and the static J- $T_{material}$ curve. It is also important to notice that $T_{applied}$ falls below $T_{material}$ at a J value of about 2700 in-lb/in² on the rapid J- $T_{material}$ curve or 3250 in-lb/in² on the static J- $T_{material}$ curve but stability was not again achieved until much later at a J of approximately 3800 to 4000 in-lb/in².

An alternative way to look at the instability and arrest process is shown in Fig 10. This figure shows the rapid load displacement data for an instability specimen and it also shows an experimentally obtained machine unloading

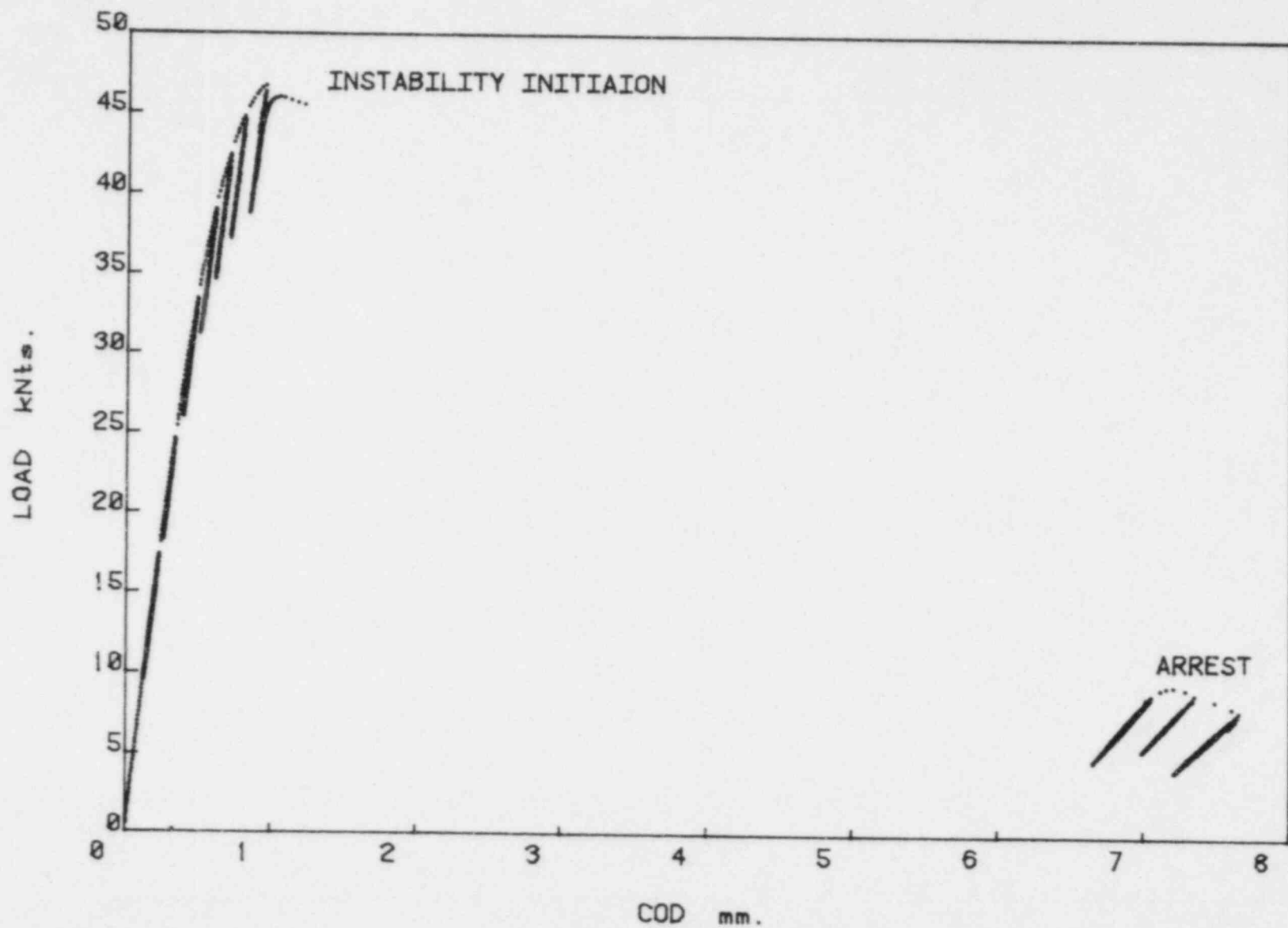


Figure 6. Typical instability data showing the usual static data defining instability and subsequent arrest.

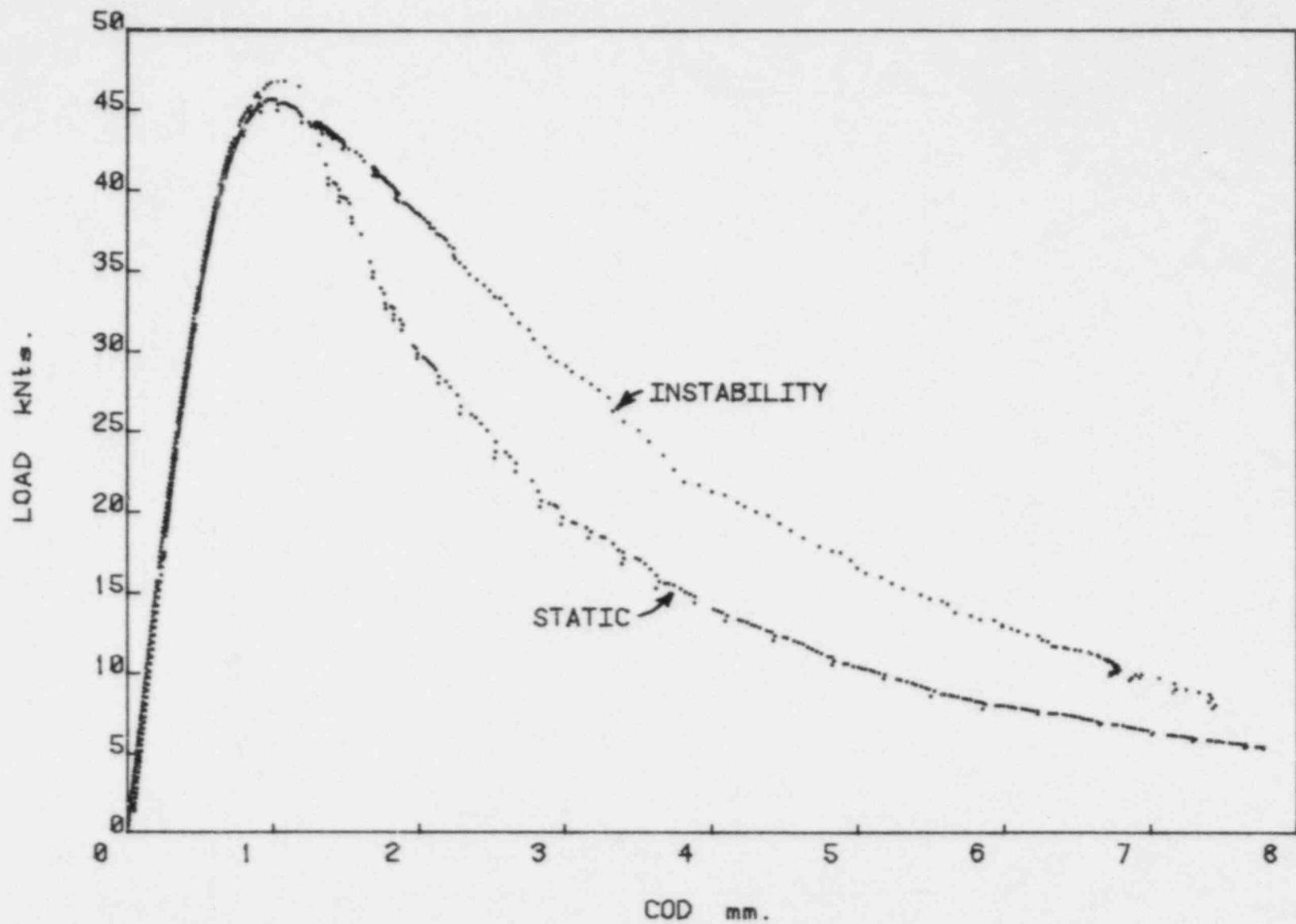


Figure 7. A combination of both static and rapid instability test data compared to baseline static load displacement data.

TABLE 2 - SUMMARY OF EXPERIMENTAL RESULTS

Specimen I.D	Test Type	Method to Predict Δa	Δa Predicted mm	Δa Measured mm	Apparatus	J Predicted at Instability kJ/mm ²	J Observed at Instability kJ/mm ²
FYBA1	Static	Unloading Compliance	13.8	13.4	Stiff Machine	-	-
FYBA2	Static	Unloading Compliance	14.0	13.8	Stiff Machine	-	-
FYBT12	Static	Key Curve k = 1558 n = 0.18	12.9	13.6	Stiff Machine	-	-
FYBT14	Static	Key Curve k = 1558 n = 0.18	13.5	14.7	Stiff Machine	-	-
FYBT11	Instability	Key Curve k = 1866 n = 0.25	12.6	12.9	$K_M = 6700$ Nt/mm	231.0	208.5
FYBT13	Instability	Key Curve k = 1866 n = 0.25	12.5	12.8	$K_M = 6700$ Nt/mm 218 Kg added mass	224.1	215.0
FYBT16	Instability	Key Curve k = 1866 n = 0.25	12.6	12.9	$K_M = 6700$ Nt/mm	252.5	240.1
FYBT18	Instability	Key Curve k = 1866 n = 0.25	12.4	12.2	$K_M = 6700$ Nt/mm 80 Kg added mass	245.2	240.0

J-R CURVES FYB INSTABILITY TESTS

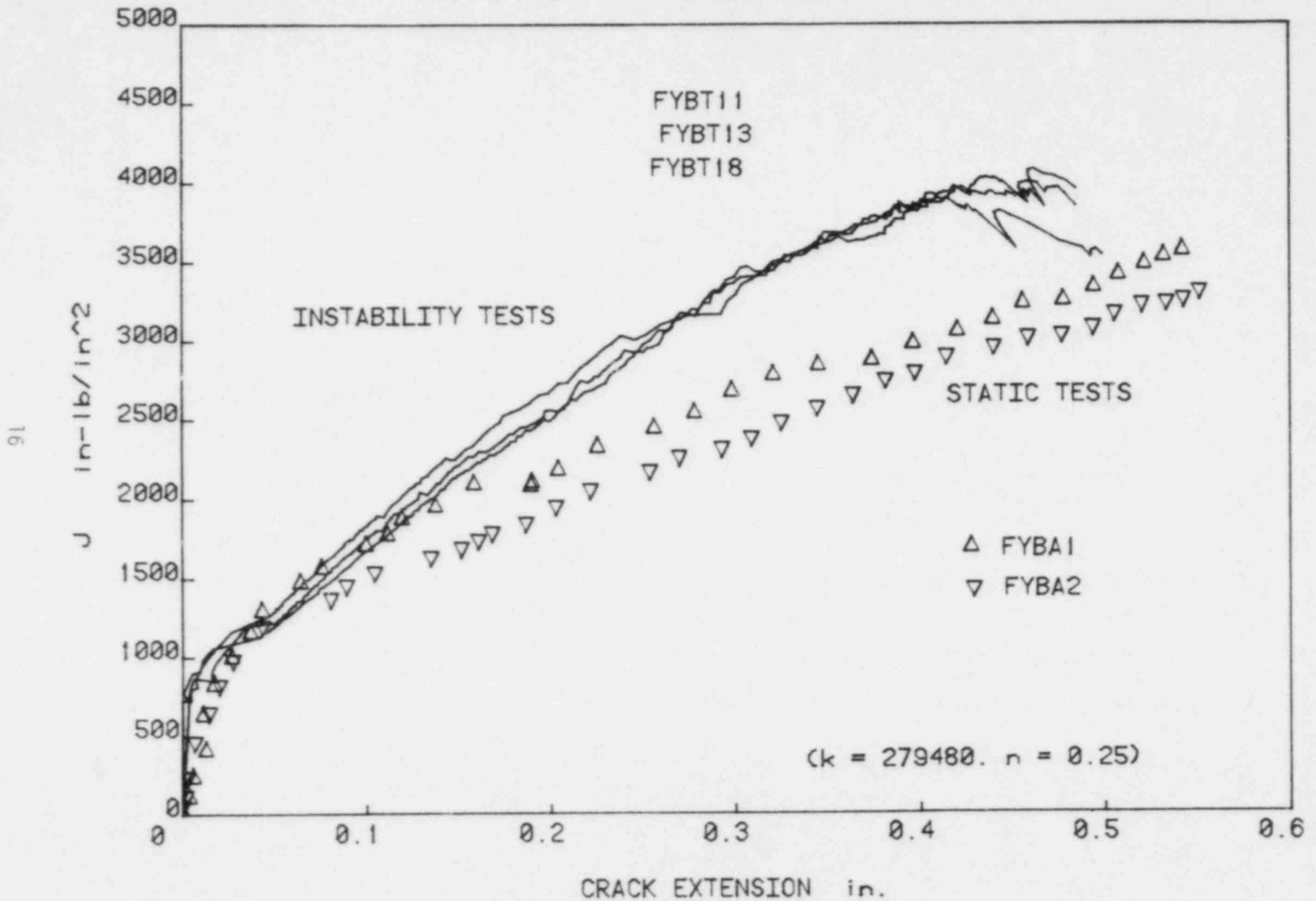


Figure 8. A comparison of tearing instability J-R curves obtained by the key curve method and baseline static J-R curves.

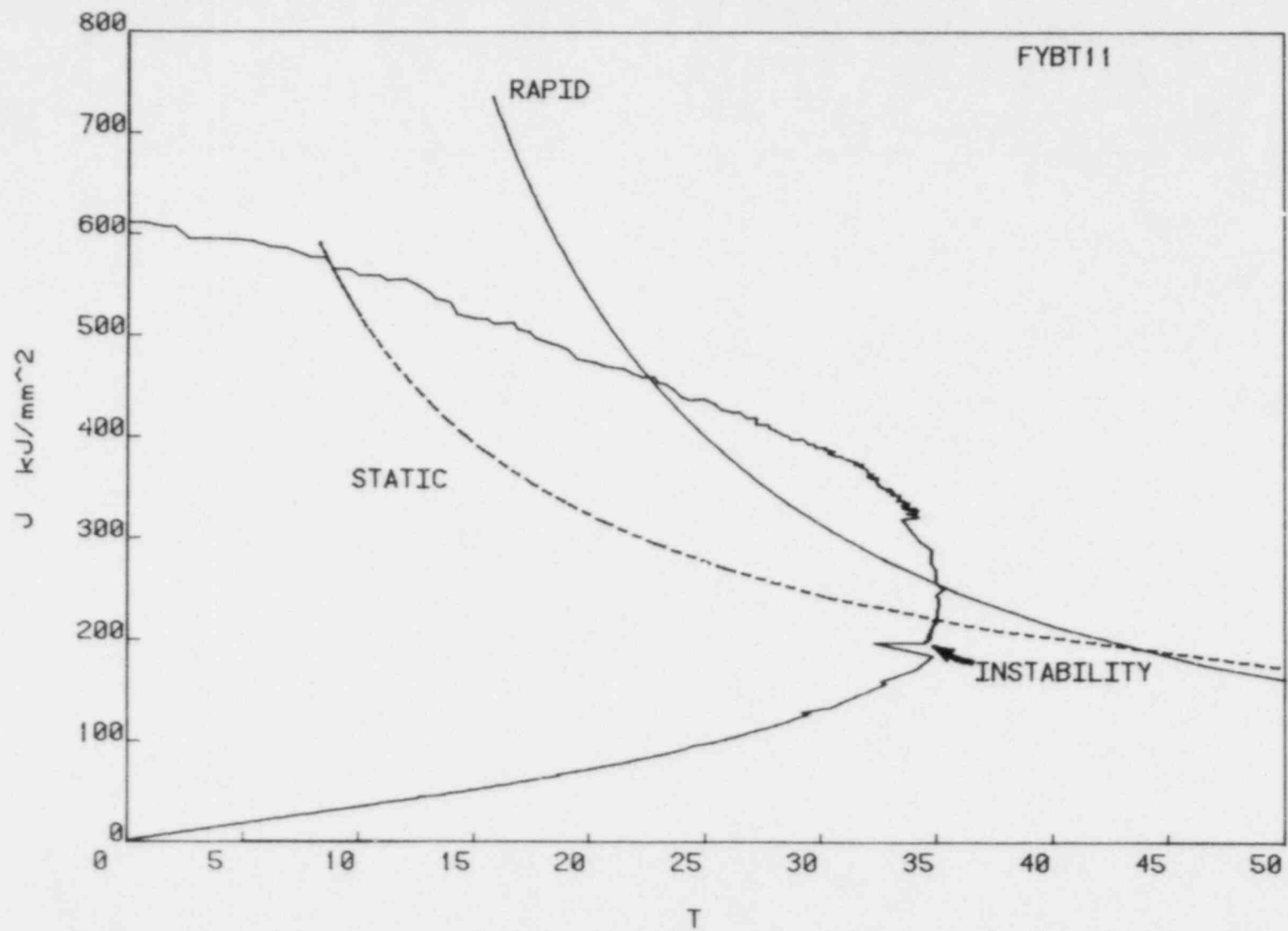


Figure 9. J-T plot showing the observed point of tearing instability.

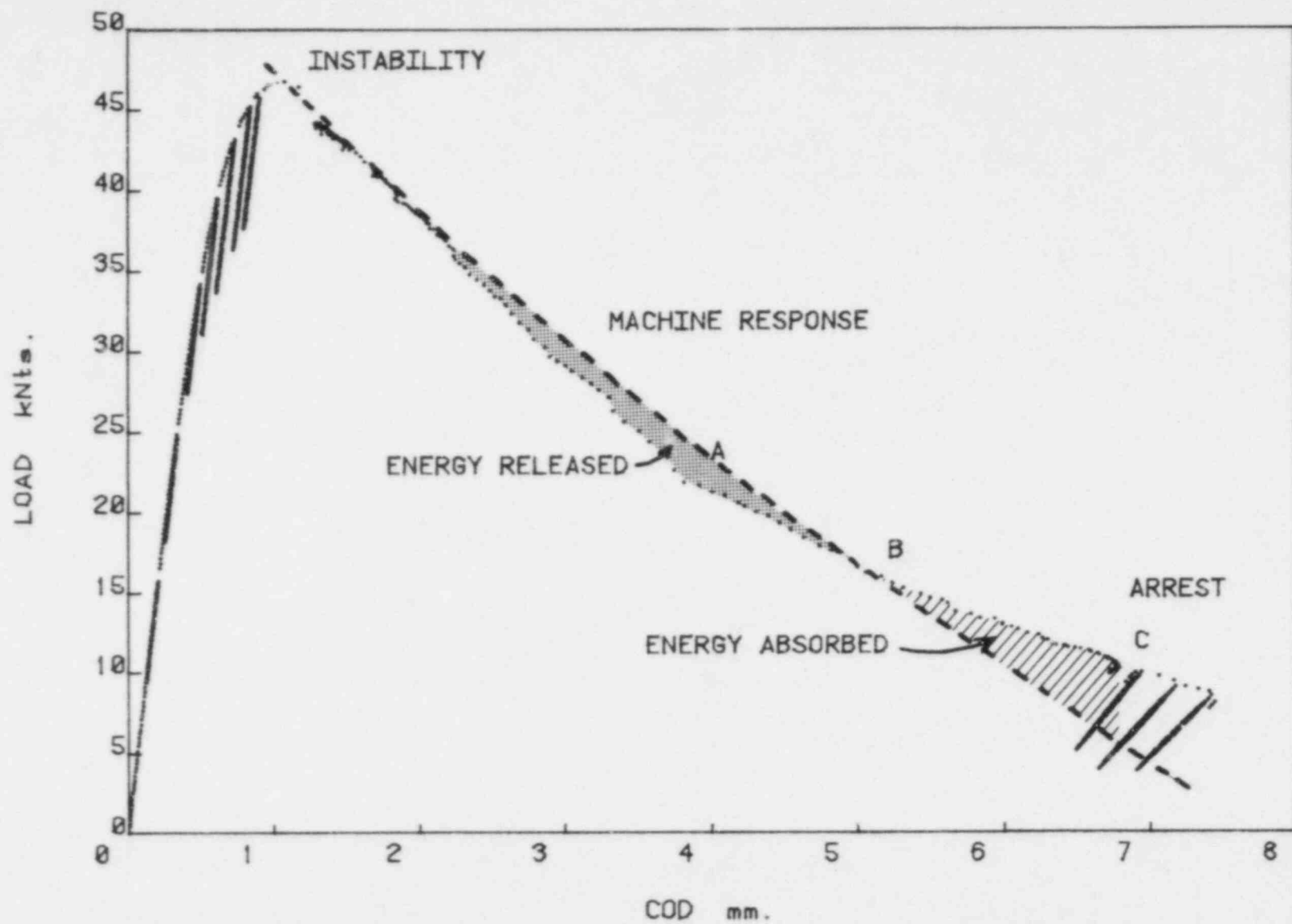


Figure 10. A load displacement plot showing the energy balance required for the arrest of a ductile tearing instability.

compliance curve shown as a dashed line. The Nicolet data obtained during the instability was collected at fixed time intervals and it is clear that the instability in fact develops rather slowly with the specimen load displacement trace initially following the machine load displacement response line. The specimen load then falls distinctly below the machine response line and a rapid acceleration occurs which continues until the specimen load displacement recrosses the machine response curve after which a deceleration occurs until arrest occurs.

Three points are labeled A, B and C on Fig 10. Point A at COD = 4mm corresponds to $\frac{dP}{d\Delta} < K_M$ at which the Ernst equations (3) (14) predict that $T_{material} > T_{applied}$.

Clearly arrest cannot occur here since the specimen load capacity is less than the load in the spring. Point B at COD = 5mm brings the specimen load capacity even with the load in the spring but arrest does not occur though $d(COD)/dt$ starts to decrease. The arrest point is at C because it is at this point that a complete energy balance is reestablished with the energy released by the spring but not absorbed by the specimen before point B is matched by the energy absorbed by the specimen in excess of what is released by the spring between points B and C.

4.0 Discussion

4.1 Conditions for Tearing Instability Arrest

The conditions for ductile tearing arrest can be stated as follows:

- 1) $T_{material} > T_{applied}$
- 2) $P_{capacity} > P_{applied}$
- 3) Energy released by spring = Energy absorbed by specimen + frictional or other absorbed energy.

4.2 Effects of Rate

Clearly rate effects play an important part in defining the point of ductile tearing arrest. If the material tested here had behaved during the instabilities as it did during static tests no crack arrest would have occurred. In this way the elevation in toughness with rate could be a very effective stabilizing effect on rapidly moving ductile cracks.

4.3 Application of Additional Mass

Application of mass to reduce the test rate was not very successful because of the large magnitude of the mass required. Application of 480 lbs (218 Kg) of mass to the system produced only the small change in COD versus time shown in Fig 11. It is important to note, however, in reference to Fig 11, that the maximum test velocity, $d(COD)/dt$, achieved corresponds to a crack velocity of approximately 20 inches per second (0.5 m/s) which is roughly equivalent to that obtained by drop tower tests and corresponds to the observed importance of material rate effects on these tests.

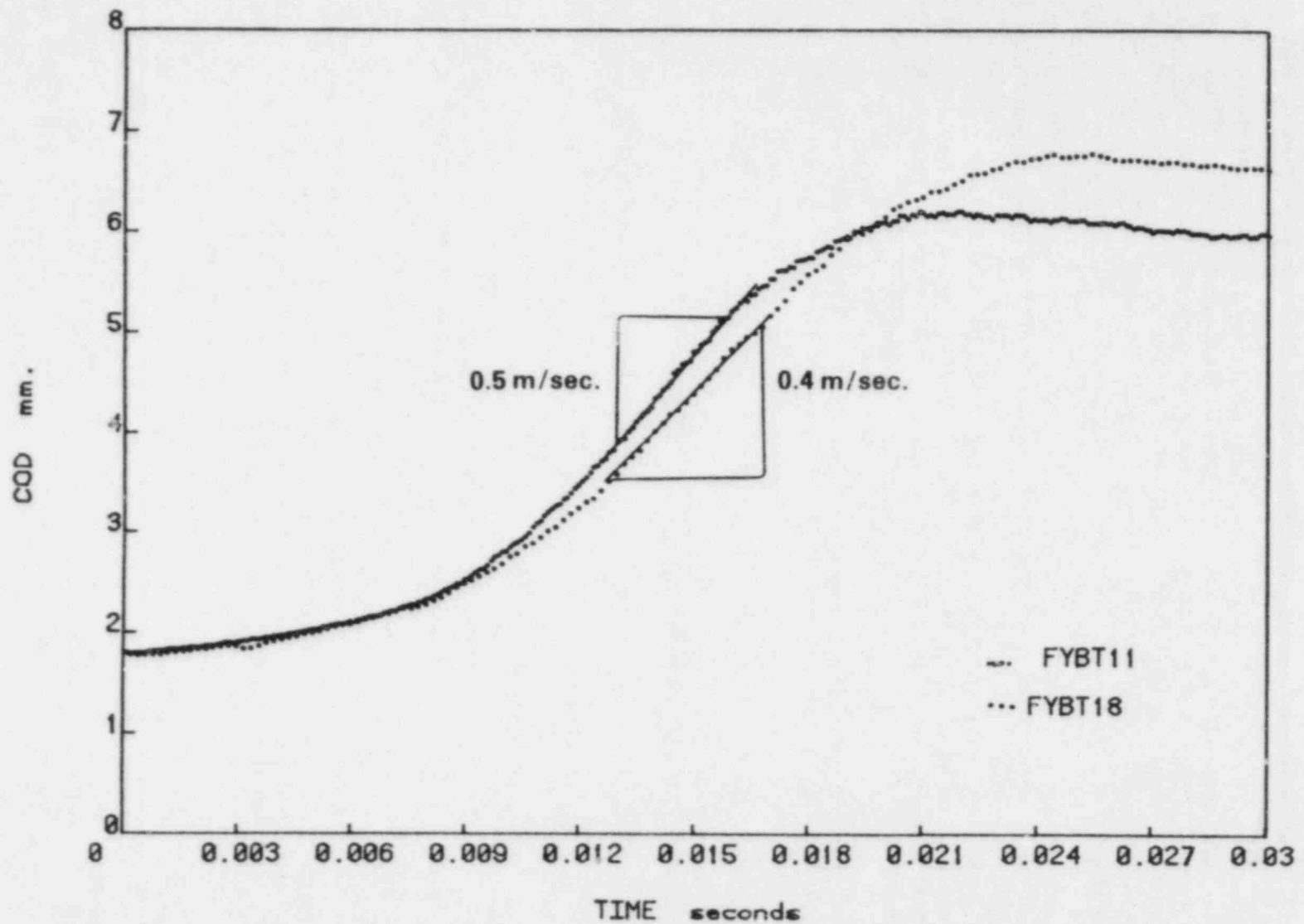


Figure 11. Plots of COD versus time shown for light and increased mass tests showing typical test velocities achieved.

4.4 Applicability of "Computer Compliant" Tests

Previous work(3) has demonstrated that a computer controlled test machine can be programmed to simulate the compliant conditions necessary to generate a ductile tearing instability in specimen or pipe geometries. These results verify that since static properties control the initiation of ductile tearing the computer system is a valuable tool for those cases where the point of instability is the major test objective. For these cases the ability of the test engineer to change the effective machine compliance by a simple keyboard command makes the test method powerful and flexible.

If the instability arrest condition is of interest, however, the computerized system is of no use whatsoever. This is so because the arrest point is strongly influenced by the rate effects of the material and the computerized system is generally very slow and controlled by the computer processor speed. Also the energy balance condition cannot be simulated on the computerized system and arrest occurs when only the first two conditions of Section 4.1 are satisfied.

4.5 Prediction of a Crack Arrest

To predict a crack arrest, i.e., the crack length at crack arrest, it is clearly necessary to accurately define the toughness properties of the material at loading rates in the vicinity of 0.5 m/s. Also necessary would be an accurate description of the elastic unloading compliance of the structure. In theory, then, it would be possible to reverse the key curve analysis to predict the structure load displacement record which if compared with the elastic structural unloading would allow prediction of the final arrest crack length. The accuracy of such an analysis would not be high but the order of magnitude of the result would give valuable insight into the likelihood of a complete separation of a critical component.

5.0 Conclusions

- An analytical key curve form fit to the load displacement curve and final measured crack length data gives accurate J-R curves directly from digital load displacement records.
- Tearing instability arrest occurs only after criterion on T, load, and energy are satisfied and rate effects are very important in setting the conditions for arrest.
- Crack velocities during tearing instabilities approach that generated in impact tests and this corresponds to the observed rate dependence of tearing instability arrest.
- It was clearly demonstrated in these results that rapid ductile crack growth produces higher loads and shorter crack lengths at a given COD (load point displacement) than occurs during the corresponding static test. In short more energy input produces a shorter crack extension during the rapid ductile crack growth spurt than occurs during a slow stable tear subjected to a smaller energy input.

Bibliography

1. Joyce, J. A., and Vassilaros, M. G., "An Experimental Investigation of the Tearing Instability Theory," Fracture Mechanics - Proceedings of the Thirteenth National Symposium on Fracture Mechanics, Richard Roberts Ed., ASTM STP 743, American Society for Testing and Materials, 1981, pp 525-542.
2. Vassilaros, M. G., Joyce, J. A., and Gudas, J. P., "Experimental Verification of Tearing Instability Phenomena for Structural Materials," Fracture Mechanics - Proceedings of the Fourteenth National Symposium on Fracture Mechanics, J. C. Lewis and G. Sines Eds., ASTM STP 791, American Society for Testing and Materials, 1983, pp 165-183.
3. Joyce, J. A., "Instability Testing of Compact and Pipe Specimens Utilizing a Test System Made Compliant by Computer Control," Elastic-Plastic Fracture, C. F. Shih and J. P. Gudas Eds., ASTM STP 803, American Society for Testing and Materials, 1983, pp II439-II463.
4. Paris, P. C., Tada, H., Zahoor, A., and Ernst, H., "The Theory of Instability of the Tearing Mode of Elastic-Plastic Crack Growth," Elastic-Plastic Fracture, ASTM STP 668, J. D. Landes, J. A. Begley, and G. A. Clarke, Eds., American Society for Testing and Materials, 1979, pp 5-36.
5. Albrecht, P., et.al, "Tentative Test Procedure for Determining the Plane Strain J-R Curve," Journal of Testing and Evaluation, JTENA, Vol. 10, No. 6, Nov 1982, pp 245-251.
6. Paris, P. C., Tada, H., Zahoor, A., and Ernst, H., "An Initial Experimental Investigation of the Tearing Instability Theory," Elastic-Plastic Fracture, ASTM STP 668, J. D. Landes, J. A. Begley, and G. A. Clarke, Eds., American Society for Testing and Materials, 1979, pp 251-265.
7. Tada, H., Paris, P. C., "Tearing Instability Handbook," NUREG/CR-1221, U.S. Nuclear Regulatory Commission, Washington, DC, 1980.
8. Tada, H., Paris, P. C., and Gamble, R. M., "A Stability Analysis of Circumferential Cracks for Reactor Piping Systems," Fracture Mechanics: Twelfth Conference, ASTM STP 700, American Society for Testing and Materials, 1980, pp 296-313.
9. Kumar, V., German, M. D., and Shih, C. F., "An Engineering Approach for Elastic-Plastic Fracture Analysis," EPRI NP-1931, Electric Power Research Institute, Palo Alto, CA, 1981.
10. Ernst, H., Paris, P. C., and Landes, J. D., "Estimation on J-Integral and Tearing Modulus T from a Single Specimen Test Record," Fracture Mechanics: Thirteenth Conference, ASTM STP 743, American Society for Testing and Materials, 1981, pp 476-502.
11. Kaiser, S., "On the Relation Between Stable Crack Growth and Fatigue," Fatigue of Engineering Materials and Structures, Vol. 6, No. 1, pp 33-49, 1983.

12. Joyce, J. A., Ernst, H., and Paris, P. C., "Direct Evaluation of J-Resistance Curves from Load Displacement Records," Fracture Mechanics: Twelfth Conference, ASTM STP 700, American Society for Testing and Materials, 1980, pp 222-236.
13. Joyce, J. A. and Gudas, J. P., "Computer Interactive J_{Ic} Testing of Navy Alloys," Elastic-Plastic Fracture, ASTM STP 668, J. D. Landes, J. A. Begley, and G. A. Clarke, Eds., American Society for Testing and Materials, 1979, pp 451-468.

ACKNOWLEDGEMENT

This study was sponsored by the U.S. Nuclear Regulatory Commission under Interagency Agreement RES-80-118. The program manager is Mr. Milt Vagins of the Metallurgy and Materials Research Branch, USNRC. Besides Mr. Vagins the author would like to acknowledge the assistance of Mr. Ed Hackett and Mr. John Gudas of the David Taylor Naval Ship Research and Development Center, Annapolis, and Mr. Mike Gibbons, Mrs. Ruth Chittum and Ms. Inez Johnson of the U.S. Naval Academy in Annapolis.

BIBLIOGRAPHIC DATA SHEET

NUREG/CR-4528

SEE INSTRUCTIONS ON THE REVERSE

2. TITLE AND SUBTITLE

Development and Verification of Conditions for Ductile Tearing Instability and Arrest

7. LEAVE BLANK

4. DATE REPORT COMPLETED

MONTH

YEAR

February

1986

5. AUTHOR(S)

James A. Joyce

6. DATE REPORT ISSUED

MONTH

YEAR

February

1986

7. PERFORMING ORGANIZATION NAME AND MAILING ADDRESS (Include Zip Code)

U.S. Naval Academy
Annapolis, MD 21402

8. PROJECT TASK WORK UNIT NUMBER

9. FUNDING OR GRANT NUMBER

B7026

10. SPONSORING ORGANIZATION NAME AND MAILING ADDRESS (Include Zip Code)

Division of Engineering Technology
Office of Nuclear Regulatory Research
U.S. Nuclear Regulatory Commission
Washington, DC 20555

11a. TYPE OF REPORT

Technical

b. PERIOD COVERED (include dates)

October 1985 - October 1986

12. SUPPLEMENTARY NOTES

13. ABSTRACT (200 words or less)

The objective of this work was to take an in depth look at the process of ductile tearing instability and especially to evaluate experimentally the conditions for arrest of a ductile tearing instability. A secondary objective was to evaluate the sensitivity of a ductile tearing instability arrest to rate at which it occurred and to the material rate sensitivity. Major conclusions are that the ductile tearing instability initiates slowly but in a mechanical spring apparatus it approaches drop tower growth rate conditions and hence the phenomena is effected by the material rate sensitivity. The conditions necessary for arrest are completely stated and demonstrated by experimental data on a 3 percent Ni structural steel.

14. DOCUMENT ANALYSIS - a. KEYWORDS DESCRIPTORS

fracture mechanics, plasticity, instability, crack growth, elastic plastic fracture, tearing instability, ductile tearing arrest, J integral, key curve method, rate effects

b. IDENTIFIERS/OPEN ENDED TERMS

15. AVAILABILITY STATEMENT

Unlimited

16. SECURITY CLASSIFICATION

(This page)

Unclassified

(This report)

Unclassified

17. NUMBER OF PAGES

18. PRICE

UNITED STATES
NUCLEAR REGULATORY COMMISSION
WASHINGTON, D.C. 20555

OFFICIAL BUSINESS
PENALTY FOR PRIVATE USE, \$300

SPECIAL FOURTH-CLASS RATE
POSTAGE & FEES PAID
USNRC
WASH. D.C.
PERMIT No. G-67

120555078877 1 1AN1RF1R5
US NRC
ADM-DIV OF TIDC
POLICY & PUB MGT BR-PDR NUREG
W-501
WASHINGTON DC 20555

INSTABILITY AND ARREST